Biomechanical wall properties of human intracranial aneurysms resected following surgical clipping

Vincent Costalat, Mathieu Sanchez, Dominique Ambard, L. Thines, Nicolas Lonjon, Franck Nicoud, H. Brunel, J.P. Lejeune, Henri Dufour, P. Bouillot, et al.

HAL Id: hal-00686616

https://hal.archives-ouvertes.fr/hal-00686616

Submitted on 24 Apr 2012

Biomechanical wall properties of human intracranial aneurysms resected following surgical clipping

(**IRRAs** Project*)

V. Costalat, M. Sanchez, D. Ambard, L. Thines, N. Lonjon, F. Nicoud, H. Brunel, J.P. Lejeune, H. Dufour, P. Bouillot, JP Lhaldky, K. Kouri, F. Segnarbieux, CA Maurage, K. Lobotesis, M.C. Villa-Uriol, C. Zhang, A.F. Frangi, G. Mercier, A. Bonafé, L. Sarry, and F. Jourdan.

* The research consortium "**I**ndividual **R**isk **R**upture **As**sessment of Intracranial aneurysm" (IRRAs) was founded by 4 clinical centers, and 3 European laboratories in France, and Spain.

Classification = Original Research

Word count: Main Text and Abstract = 2829

BM-D-11-00205

Contact information:
Vincent Costalat, MD, PhD (vincentcost@hotmail.com)
CHU Montpellier, Interventional Neuroradiology, Av Augstin Fliche, Montpellier, France.

1

27

28

All authors have made substantial contributions to all of the following:

    (1) the conception and design of the study; VC;DA;FJ;FN;MS

    (2) acquisition of data; VC;MS; LT;NL;JPL;FS;HD;HB;PB;JPH;CAM;KK;AB

    (3) analysis and interpretation of data; GM;VC;FJ;DA;MS

    (4) drafting the article or revising it critically for important intellectual content;
      VC;MS;FJ;KL;DA;FN;LS;AFF

35

2

35

36

37

38

Abstract:

Background and Purpose— Individual rupture risk assessment of intracranial aneurysms is a major issue in the clinical management of asymptomatic aneurysms. Aneurysm rupture occurs when wall tension exceeds the strength limit of the wall tissue. At present, aneurysmal wall mechanics are poorly understood and thus, risk-assessment involving mechanical properties is inexistent. Additionally, aneurysmal computational hemodynamics usually makes the assumption of rigid walls, an arguable simplification. We therefore aim to assess mechanical properties of ruptured and unruptured intracranial aneurysms in order to provide the foundation for future patient-specific aneurysmal risk assessment. This work will also challenge some of the currently held hypotheses in computational flow hemodynamics research.

Methods—A specific conservation protocol was applied to aneurysmal tissues following clipping and resection in order to preserve their mechanical properties**. Sixteen intracranial** aneurysms (11 female, 5 male) underwent mechanical uni-axial stress tests under physiological conditions, temperature, and saline isotonic solution. These represented 11 unruptured and 5 ruptured aneurysms. Stress/strain curves were then obtained for each sample, and a fitting algorithm was applied following a 3-parameter (C^{10}, C^{01}, C^{11}) Mooney-Rivlin hyperelastic model. Each aneurysm was classified according to its biomechanical properties and (un)rupture status.

Results— Tissue testing demonstrated three main tissue classes: Soft, Rigid, and Intermediate. All unruptured aneurysms presented a more Rigid tissue than ruptured or pre-ruptured aneurysms within each gender subgroup. Wall thickness was not correlated to aneurysmal status (ruptured/unruptured). An Intermediate subgroup of unruptured aneurysms with softer tissue characteristic was identified and correlated with multiple documented risk factors of rupture.

Conclusion: **A significant biomechanical properties modification between ruptured aneurysm, presenting a soft tissue and unruptured aneurysms, presenting a rigid material was observed. This finding strongly supports the idea that a biomechanical-based risk factor can and should be developed in the near future to improve the therapeutic decision making.**

4

68

69

Introduction:

The prevalence of unruptured intracranial aneurysms in the general population, as reported by a recent review,[1] ranges between 3% and 6.6%. The incidence of ruptured aneurysms is however, low, with approximately 0.5% per year suggesting that very few aneurysms rupture. Subarachnoid hemorrhage is the consequence of aneurysm rupture and approximately 12% of patients die before receiving medical attention, 40% of hospitalized patients die within one month after the event, and more than one third of those who survive have major neurological deficits. In contrast endovascular treatment of unruptured aneurysms is safe with less than 1% mortality rate[2]. Unruptured intracranial aneurysms represent a dilemma for the physicians. The risks of aneurysm rupture with respect to its natural history against the risk of morbidity and mortality from an endovascular or surgical repair has to be carefully balanced. With brain imaging being more frequently and widely used, a growing number of intracranial aneurysms are being diagnosed, posing the problem of which aneurysms harbor a sufficiently high risk of rupture to merit endovascular or surgical repair. Recent publications have addressed this issue and have demonstrated that, among other variables affecting the natural history of aneurysms, aneurysm size and location represent independent predictors of rupture risk [3]. Other parameters, such as irregular aneurysm shape and, in particular, the presence of blebs[4, 5] are recognized as high risk factors.

Rupture of an aneurysm occurs when wall tension exceeds the strength limit of the wall tissue. The ideal approach to risk assessment would therefore be to determine tension and material strength limits of the tissue[6] in the aneurysmal wall. Individual aneurysmal material strength is impossible to measure non-invasively, but wall tension can be estimated using computational simulation[7]. Over the last decade, a number of authors have shown that computational fluid dynamic simulations based on patient-specific anatomical models derived from medical imagery may be used to assess wall shear stress (WSS) and pressure in the Circle of Willis[8] [9, 10]. Others have used the same approach to analyze cerebral aneurysms, with particular focus on WSS, which is thought to be associated with aneurysm formation and risk rupture.[11] [12, 13] Although simulation of aneurysmal wall tension is now feasible in principle, real human aneurysmal wall biomechanical properties are still rarely explored in the literature.[14, 15] Computational simulations must be based on reliable material properties and

boundaries. As opposed to hemodynamic boundary conditions that may be assessed by Phase Contraste-MRI or transcranial Doppler, in vivo, patient specific measurements of tissue properties are not feasible yet. .Most of the current research on computational hemodynamics assumes uniform wall thickness and wall properties based on average values extracted from the scarce available literature. Although some of these assumptions may be acceptable in practice, no in-depth study has demonstrated their validity thus casting shadows on the accuracy of the current computational hemodynamics work. For this purpose a research consortium (**IRRAs** for **I**ndividual **R**isk **R**upture **As**sessment of Intracranial Aneurysm) was founded between 3 research Laboratories and 4 French neurosurgical centers (Montpellier, Lille, Nimes and Marseille) and involving corresponding departments of neuroradiology and anatomopathology. The first purpose of the **IRRAs** consortium is to build a database of aneurysmal biomechanical parameters. Such database will be instrumental in supporting new computational strategies to determine the risk of rupture in cerebral aneurysms based on patient-specific imaging data and domain-specific biomechanical knowledge.

The purpose of this study is to explore the biomechanical behavior characteristics of ruptured and unruptured aneurysms. Building such database is a mandatory to establish the idea that the rheology of the tissue correlates with the status of the aneurysm and that a biomechanical-based risk rupture factor can indeed be developed.

Materials and methods

Surgical technique and aneurysm selection

Eighteen patients treated for ruptured or unruptured aneurysms by surgical clipping were recruited by 4 French neurosurgical teams. The research study protocol was approved by the local ethical committee in each center. A consent form was signed by patients with normal neurological status, or by the relatives in all other cases. Following surgical clipping (Fig.1) angio fluoroscopy imaging was performed by the neurosurgeon to control aneurysm sac exclusion. Once the distal aneurysm was confirmed to be safely excluded from the circulation, the neurosurgeons removed it in one piece. In this way, 18 intact aneurysms samples were then extracted from 17 patients.

Clinical and Radiological Data

For each patient, clinical, and radiological information was collected concerning age, gender, aneurysm status (ruptured/unruptured), size (measured from the dome of the aneurysm and the neck represented by the communication of the aneurysm with the parent artery), the "dome to neck" ratio (aneurysm size/neck length), location on the Willis circle, morphological evaluation (classified "simple shaped" for regular unilobulated aneurysm and "complex shaped" for multilobulated and irregular aneurysm), as well as documented rupture risk factors; multiple aneurysms, previous ruptured aneurysm, positive family history of ruptured intracranial aneurysm, autosomal dominant polycystic kidney disease, hypertension, alcohol and tobacco. A possible mycotic intracranial aneurysm etiology was considered an exclusion criterion, as well as any previous history of endocarditis and inflammatory disease. **All documented risk factors were then recorded in order to be related to the biomechanical behavior of each aneurysm.**

Aneurysm Sample Conservation protocol

In order to conserve the mechanical properties of the aneurysm wall, a specific conservation protocol was applied in each center by means of a dedicated histopathological removal kit available in the neurosurgical operating room. The resected aneurysm was initially inserted in a tube containing a Ringer lactate, 10% DMSO solution. This first tube was then placed in a larger second one containing isopropanol. This combination of the two tubes was placed in a freezer (-80°C). The sample was progressively frozen due to the surrounding isopropanol solution in order to maintain its biomechanical properties[16]. Frozen samples were then stored in

150 the anatomopathology department of the neurosurgical center, before mechanical testing was

151 carried out.

152

Biomechanical testing methodology

154 One hour before mechanical testing, aneurysms sample were thawed at ambient temperature.

155 Under microscopy, the aneurysmal wall samples were dissected in a meridional manner in

156 order to obtain a regular rectangular piece (Fig.2). **Only the meridional axis of the**

157 **aneurysm was chosen in order to preserve maximum length of the aneurysmal tissue in**

158 **the sample given the very small size of each specimen and the fragility of the tissue.** The

159 aneurysm strips were physically measured and then glued on each extremity to aluminum

160 grips. Meanwhile, physiological isotonic liquid was warmed to 40°C inside the traction test

161 machine. A uniaxial stretch test was carried out on the sample within the warmed

162 physiological liquid in order to simulate the in vivo conditions (Fig. 3a). This testing device

163 was composed of a Texture Analyzer (TA-XT2, Stable Microsystems, UK) with a 50 N load

164 cell and an optical microscope (ZEISS) equipped with a digital video camera .

165 The uniaxial stretch test consisted of a sequence of 10% length displacement of the sample, in

166 5 repeated cycles (Fig. 3b), while registering the traction force applied. This 10% value was

167 initially calculated by Karmonik et al.[17] in an in-vivo wall motion MRI study of 7 aneurysms**.**

168 **In accordance to standard mechanical testing protocol for biological tissue, the speci-**

169 **mens were first preconditioned[18] during the first four cycles.**.The extension rate was 0.01

170 mm/s and the tension load was recorded every 0.01 s. Velocity of the solicitations was small

171 enough to not consider viscous phenomena. A baseline tension of 0 Newton was applied to

172 the strip before starting each test, and two cameras were orthogonally placed and focused on

173 the sample after a calibration test

174 During the test, the two subset cameras were used to record the displacement of the sample.

175 These images were subsequently used to determine the exact **dimensions** of the strips (resolu-

176 tion of 4μm/pixel). A Force/Displacement graph was obtained **from each sample testing al-**

177 **lowing tissue characterization**

178

8

Post processing

179 Only the measurements from the last elongation cycle were used in order to obtain more real-

180 istic mechanical characterization of the data. Note however that except for the very first cycle,

181 the force/displacement graph was roughly cycle independent (fig 3 b).. In order to tune the

182 parameters of an equivalent hyperelastic model, the force/displacement graph described

183 above was converted in a strain/stress graph. For this calculation, the length, thickness and

184 width of each strip were considered (Fig. 3b). A baseline for this aneurysmal **strip dimen-**

185 **sions** were obtained at 0-Newton traction in the third cycle of each test. Using the assumption

186 that the specimen was subjected to a uniform traction and presented a constant section during

187 the test, the Cauchy stress was computed, and the engineering strain registered[19, 20].

188 During the cycles some permanent deformation in the traction phase was observed causing

189 slight compression of the sample in the rest phase. This is reflected by the negative values of

190 the curve origin in Figure 3b and is in accordance to the elasto-plastic behavior of the tissue.

191 Since we consider an hyperelastic model to represent the tissue, the (moderate) plastic effects

192 cannot be represented and only the positive part of the curve was used to identify material

193 behavior.

194 Once the strain/stress graph was obtained, we proceed to a mathematical matching using a

195 Sequential Least Squares Programming algorithm in order to determine the corresponding

196 hyperelastic model and its coefficients. In our cases, the best match was obtained with a 3

197 parameters Mooney-Rivlin model[21, 22]. Let F be the measured load, S_0 the initial section and λ

198 the elongation of the sample, the behavior law is given by equation (1)..

199   (1) $\dfrac{F}{S_0} = 2(\lambda - \lambda^{-2})\left(c_{10} + c_{01}\lambda^{-1} + c_{11}(3\lambda^{-2} + 3\lambda - 3 - 3\lambda^{-1})\right)$

200   where the material parameters are C_{10}, C_{01} and C_{11}. The values of each of these

201   coefficients for each aneurysm are gathered in Table 1 together with **strip dimensions**

202   and relevant clinical factors.

203 **Statistical analysis**

204 The aneurysmal wall characteristics were presented using median and range for continuous

205 variables and frequencies and proportions for categorical variables. Groups (defined by

206 biomechanical status and material property) were compared using non-parametric Wilcoxon

9

207 rank test for continuous variables and Fisher exact test for categorical ones. Statistical

208 significance threshold was set at 5%. Statistical analyses were performed using SAS version

209 9.1 (SAS Institute, Cary, North Carolina).

210

211 **Results:**

212 *Population:*

213 Eleven unruptured and five ruptured aneurysms were included in the study. In one unruptured

214 aneurysm case, pre-rupture symptoms with acute headache, and recent vision loss secondary

215 to optic nerve compression was reported and highlighted in the table 1. Mean age was 46.7

216 (min 32 – max 64). Location was middle cerebral artery (MCA) in 9 cases (56.6%), anterior

217 communicant artery (AComA) in 3 cases (18.7%), posterior communicant artery (PComA) in

218 2 cases (12.5%), and internal carotid artery (ICA) in 2 cases (6%). Aneurysm size is ranging

219 from 4.2 to 13 mm.

220 *Sample and Mechanical testing:*

221 Out of the 16 surgically clipped aneurysms that were subjected to mechanical uniaxial strain

222 tests, 11 were from female and 5 from male patients (Sex Ratio = 0.45). Mean strip length

223 was 4.8 mm (ranging from 1.3 to 8), with a mean thickness of 370 μm (ranging from 170 to

224 680 μm), and a mean section surface of 0.62 mm^2 (ranging from 0.29 to 1.6 mm^2).

225 The coefficient C_{10} value ranged from 0 to 0.9 Mpa with a mean value of 0.19 Mpa, C_{01}

226 ranged from 0 to 0.13 Mpa with a mean value of 0.024, C_{11} ranged from 0.124 to 32 Mpa

227 with a mean value of 7.87.

228 To facilitate analysis, aneurysms were classified according to their status Rup-

229 tured/Unruptured and their biomechanical behavior Rigid/Soft/Intermediate (see Tables 1 and

230 2).

231

232 *Comparison of biomechanical parameters value among ruptured and unruptured aneu-*

233 *rysms are summarized in tables 3, 4, and 5.*

234

235

236

237

238 **Discussion**

239 *Results analysis*

10

240   A recent case-control study [23] on 4000 patients based on genetic variation suggests

241   that the underlying mechanism for intracranial aneurysm pathogenesis may differ between

242   male and female subjects, underlining the importance of a stratified analysis between genders.

243   A significant difference in biomechanical parameters between ruptured and unruptured aneu-

244   rysms was observed in our data within each gender group (Tables 3, 4, 5), therefore support-

245   ing the above statement.

246   Interestingly, the C_{11} coefficient, which represents the main curvature of each graph was the

247   most representative parameter of this observed biomechanical difference (Table 3, $p<0.004$).

248   The first two coefficients C_{01}, C_{10} presented a low value (near 0) and were not significantly

249   different ($p=0.4$ and $p=0.7$) regarding aneurysmal status (ruptured/unruptured). All C_{11} values

250   were observed below 1.2 MPa (mean 0.37 MPa) in ruptured or pre ruptured female aneu-

251   rysms, and below 3.2MPa (mean 3.1MPa) in male ruptured aneurysms.

252   In the female group, all the unruptured aneurysms presented a more rigid behavior

253   than the ruptured or pre-ruptured aneurysms ($C_{11} = 0.48$ vs 11.7 MPa; $p<0.001$, Table 4). Be-

254   tween the unruptured aneurysms, we can distinguish two subgroups; the Unruptured/Rigid

255   patients (#2-#7-#9) and the Unruptured/Intermediate patients (#8-#10-#11-#15). In this last

256   subgroup representing an unruptured aneurysm with a softer aneurysmal wall, three out of

257   four presented either documented major epidemiologic risk factors or a radiologically high

258   risk shape (multilobulated). Only one aneurysm (#15) was simple shaped without further as-

259   sociated risk factors in this subgroup. One single patient (#16) presenting an unruptured aneu-

260   rysm was classified as Soft with similar material properties with the Ruptured group. In this

261   particular case, pre-rupture symptoms with major headache, and recent optic nerve compres-

262   sion were recorded few days before surgery and motivated urgent treatment. Therefore, in this

263   case, the mechanical test findings of Soft may not be as paradoxical as thought of at the first

264   glance.

265   In the male group, all the unruptured aneurysms tended have Rigid material than the

266   ruptured ones ($C_{11} = 11.95$ vs 3.17 MPa; $p=0.058$, Table 5). Similarly to the female, unrup-

267   tured aneurysms can be split in two subgroups, with 2 aneurysms classified Unrup-

268   tured/Intermediate (Aneurysm #12 and #14), and one aneurysm classified Unruptured/Rigid.

269   Among the Intermediate/Unruptured aneurysms one presented a major documented risk factor

270   with multiple aneurysms, in accordance to a possible underlying connective tissue disease.

271   Interestingly, in the male group, the ruptured aneurysms (Aneurysms #5 and #13) had a

272   thicker wall compared to the Intermediate/Unruptured aneurysms, in contradiction to common

273   conceptions, and in accordance to previous histoptaholomic work[24].

11

274 **Rheological data relevant to aneurysmal tissue are very scarce in the literafture.**

275 **To the authors' knowledge, the only previous study is by Toth et al. [22] who also gained**

276 **insights about the tissue rheology from 1D traction testing. Unfortunately, no subgroup**

277 **analysis among ruptured or unruptured status was performed by Toth et al. and the**

278 **significant parameter C_{11} was not calculated. Still, the initial mean tangent modulus they**

279 **obtained for their hyerelastic model can be compared to the $C_{01}+C_{10}$ parameter from the**

280 **previous study. For the women group, this initial tangent modulus was evaluated from**

281 **2.79 10^{-2} to 22.4 10^{-2} Mpa vs whereas it is in the range 1.905 10-2 to 77.05 10-2 in our**

282 **study. For the men group, this value was measured from 2 10^{-2} to 25.3 10^{-2} Mpa vs**

283 **from 10.15 10^{-2} to 93.74 10^{-2} in our study.** From the results presented in this study, re-

284 producible material characteristics were observed among the ruptured and pre-

285 **ruptured aneurysms with similar biomechanical behavior, suggesting a same vulnerable**

286 **status of the aneurysmal wall in a rupture or pre-rupture status. These two behaviors**

287 **were significantly different from the unruptured aneurysms, presenting a rigid tissue.** At

288 the same time, there was no statistical correlation observed between the thickness of the wall,

289 the aneurysm size and the Ruptured/Unruptured aneurysms status. This observation supports

290 the hypothesis that the aneurysm wall vulnerability is directly related to the tissue microstruc-

291 ture[25], and not to a progressive wearing of the wall.

292 The evolution of aneurysmal biomechanical properties was modeled by Watton et al.et

293 al.[26] who performed numerical simulations of aneurysmal initiation and growth and postulated

294 a degradation model of the elastin layer. Furthermore, a previous histopathology study[25] dem-

295 onstrated that prior to rupture, the wall of cerebral aneurysm undergoes morphological

296 changes associated with degeneration and repair.

297 **The main contribution of our study has been to demonstrate a very significant**

298 **biomechanical property difference between pre-rupture or rupture aneurysms with a**

299 **soft tissue and unruptured aneurysm with a Rigid tissue** (Fig.6).

300

12

300

301

302

Limitation of the study

Because of the surgical resection necessary to obtain these samples, only aneurysms easily and safely accessible were selected, introducing a potential selection bias in this study. Hence, the MCA location was over-represented. There may be also a bias induced by the differences between cases with indication of surgical treatment compared to those indicated for interventional therapy. Nevertheless we observed aneurysm size ranging from 4.2 to 13 mm representing the majority of aneurysms treated to date. Within the statistical limitations of our sample, we could not observe any significant difference in mechanical properties of the aneurysmal wall according to the location. Interestingly, in the patient harboring two aneurysms (aneurysm #10 and #11) in different locations (ICA and MCA, respectively), we observed similar mechanical properties.

Uniaxial strain/stress testing is not representative of the anisotropic behavior of the aneurysm wall in vivo. **Although, bi-axial testing was contemplated in this study, it is technically challenging to carry out. In our experiments the main limitation was the small size of the strips ranging from 1.2 to 8 mm. Work by Toth et al.[15] also confirms that bi-axial testing does not generate reliable and reproducible results**. MacDonald et al.[30] investigated the molecular strength of the collagen fibers layers in 4 aneurysms. When comparing directional tissue strength, an anisotropy was demonstrated by a factor of 2. **In our study, aneurysm samples were selected in a meridional direction in both groups demonstrating a difference between ruptured and unruptured aneurysm in this direction. A bi-axial testing of the sample would have been a response to this high level of anisotropy, but these tests were not possible in our experience due to the very small size of the aneurysms.**

Furthermore, the probability of consistently and systematically slicing the aneurysm sample in the weakest direction in the ruptured aneurysms, and the strongest direction in unruptured aneurysms was unfeasible.

Conclusion

Gender stratification was necessary to interpret the biomechanical testing. Within each gender subgroup; ruptured aneurysms presented lower Rigidity than ruptured aneurysms, supporting the hypothesis that there is a change in the biomechanical properties of the aneurysm wall

13

333 preceding rupture. Secondly, wall thickness was not correlated to ruptured/unruptured status.

334 An Intermediate subgroup of unruptured aneurysms characterized by material properties cor-

335 responding to softer tissue was identified, and associated with multiple well documented risk

336 factors of aneurysm rupture. Further studies about the biomechanical properties of cerebral

337 aneurysms can help elucidating the biomechanical conditions preceding rupture. With the

338 recent progress in *in vivo* aneurysm wall motion estimation[17, 31] it may be possible soon to

339 estimate *in vivo* mechanical material properties of cerebral aneurysms[32, 33]. Such biomechani-

340 cal parameters might be themselves good predictors of aneurysm rupture or might be inte-

341 grated within a more comprehensive pipeline for image-based patient-specific simulations of

342 fluid-wall structure interaction that renders a personalized estimate of the presence of vulner-

343 able aneurysmal wall tissue and a potential increased rupture risk.
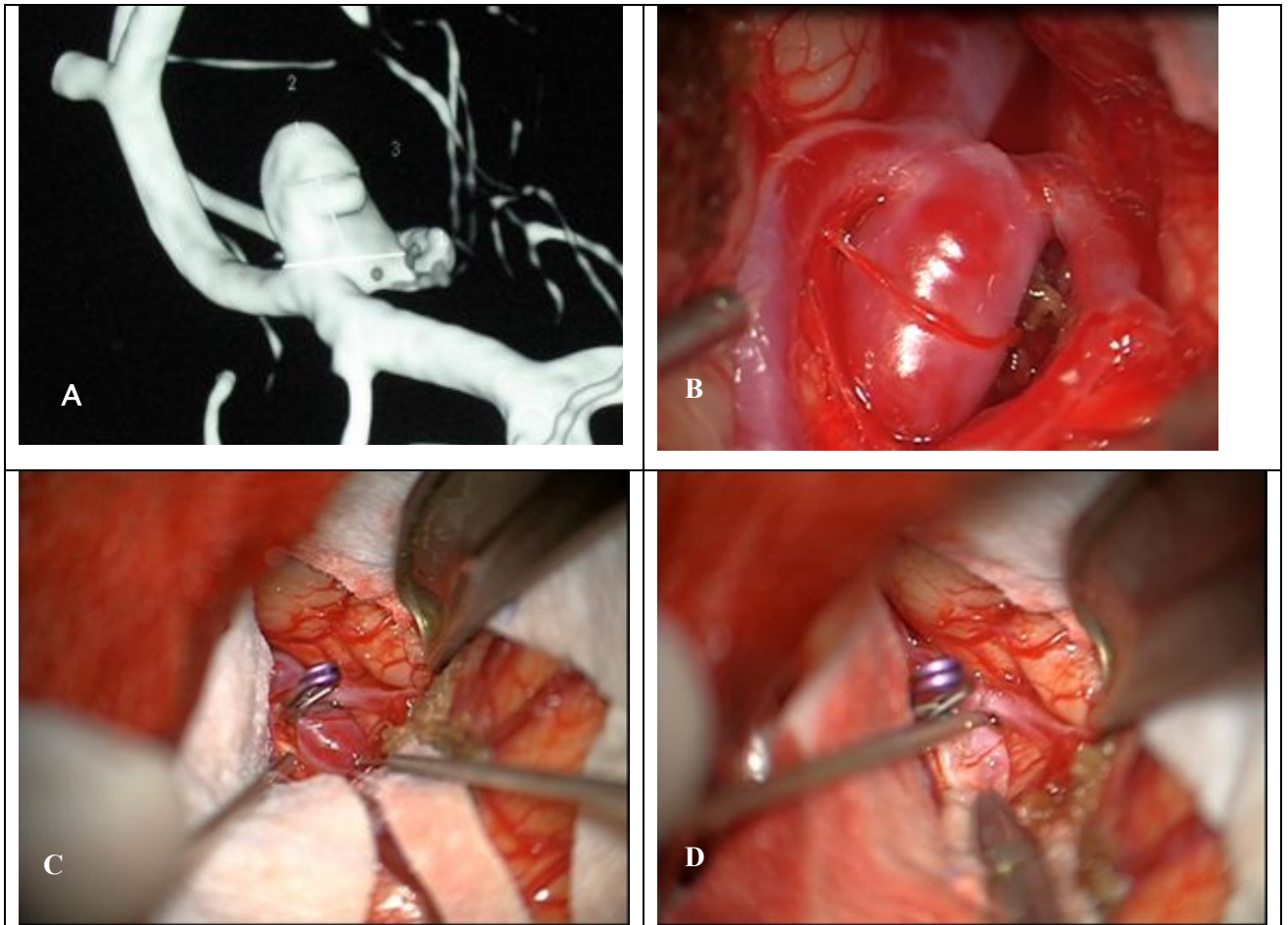
344

345

345

346

347

Fig. 1. (A) Three-dimensional rotational angiography imaging from Aneurysm #9. (B) Surgical view of this aneurysm in Middle Cerebral Artery location before clipping. (C)Aneurysm sac after surgical clipping. (D) Aneurysm resection.

348

349

349
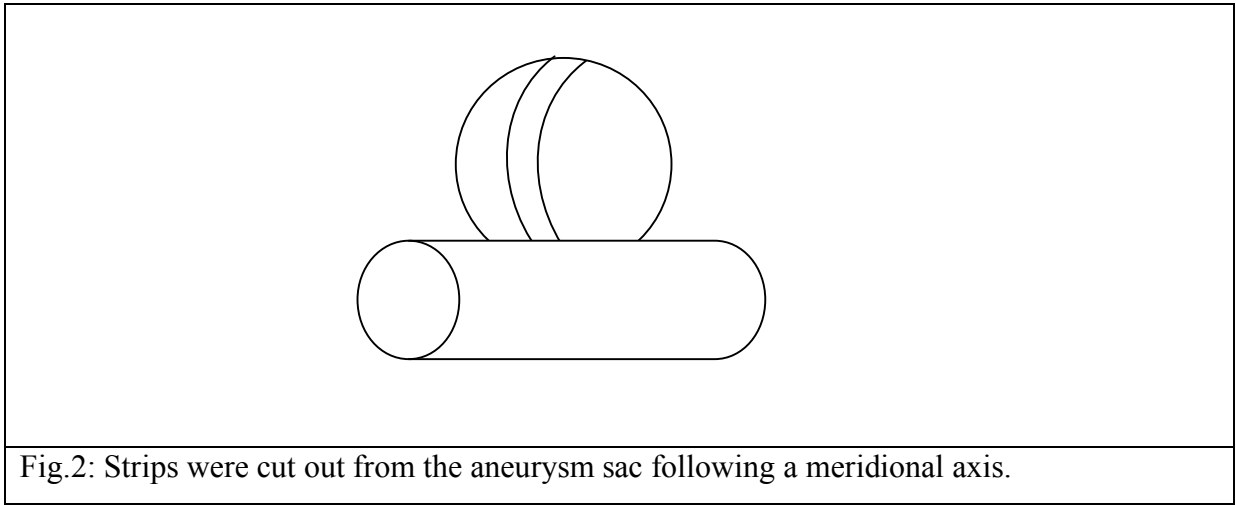
Fig.2: Strips were cut out from the aneurysm sac following a meridional axis.

350

351

16

A.	
B.	

Fig.3: Set-up and results from the uni-axial biomechanical testing. A. Side view of a wall strip from aneurysm n°4 during strain test, in a Ringer Lactacte solution at 40°C. B. Strain/Stress graph. The hysteresis is observed between the first load (*) and the five cycles. **A slight compression was observed during the rest phase due to micro structural changes of the sample during the first cycles leading to a permanent elongation. When coming back to initial size of the sample, a slight compression is then observed on the graph (arrow).**

353

354 <u>Fig. 4:</u> Plots of the strain/stress relationships measured for men (R=ruptured, U=unruptured,

355 ACA = Anterior Cerebral Artery, ACM=Middle Cerebral Artery)

356

357
358
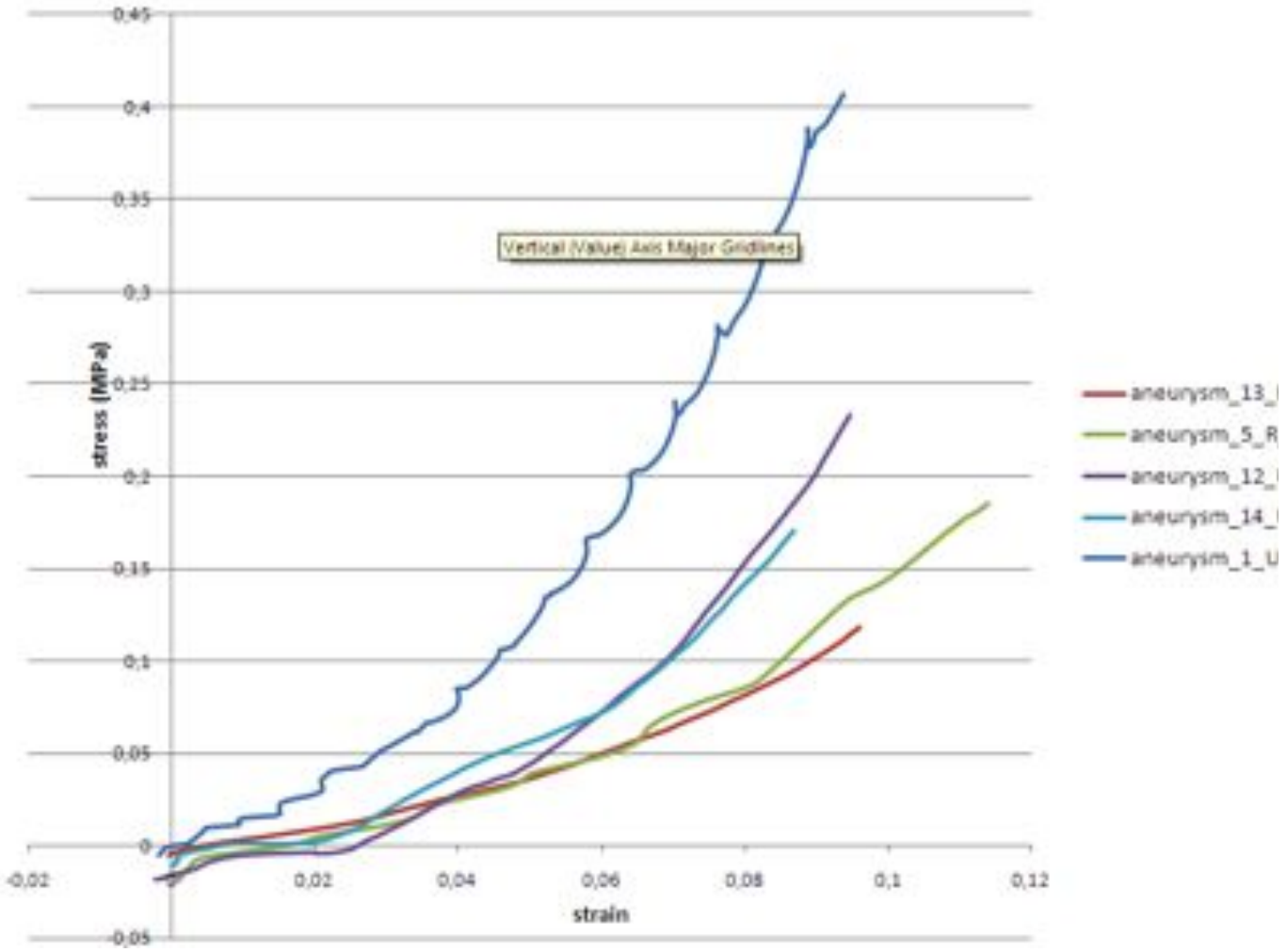359
360
361
362
363
364
365
366
367
368

18

369
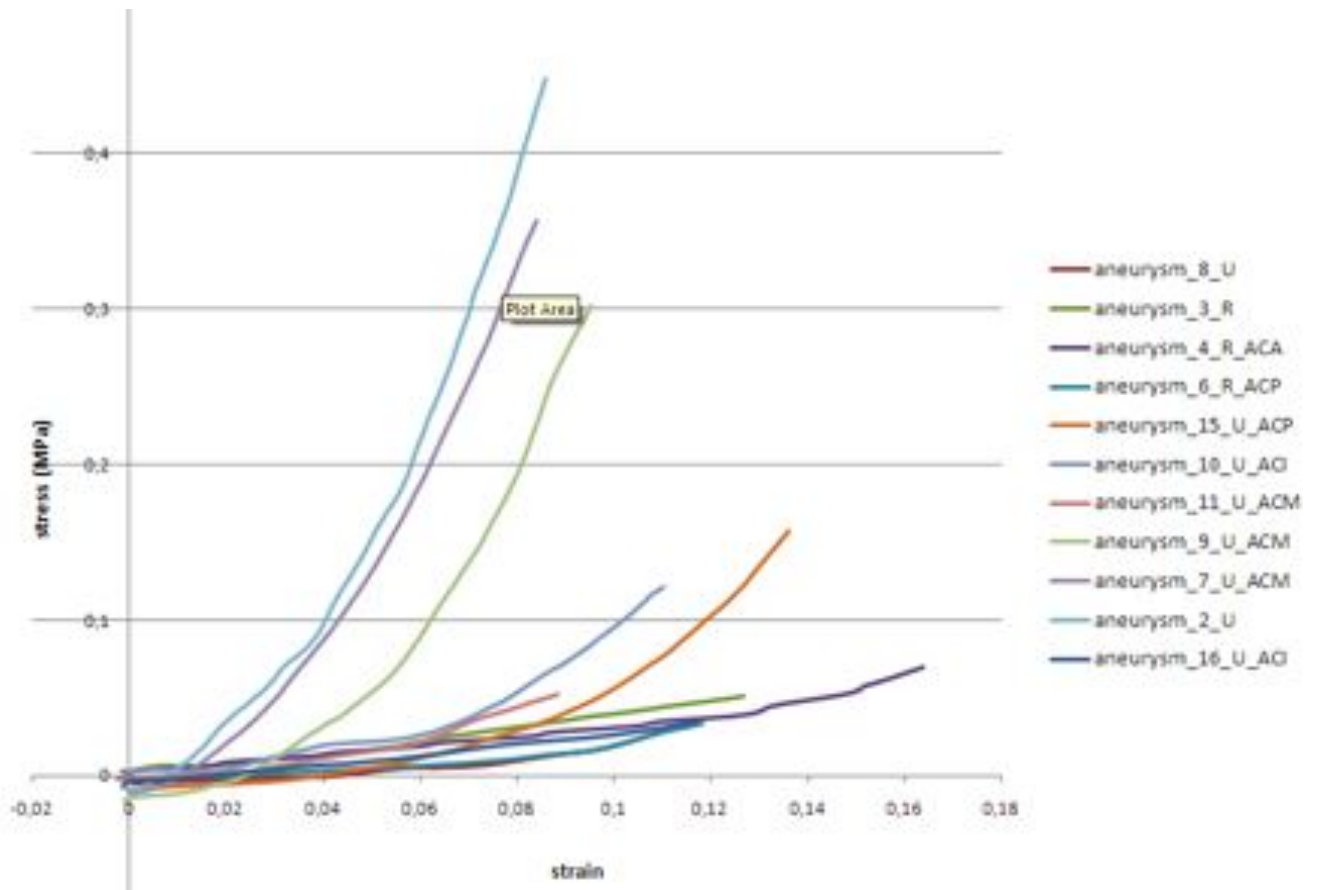
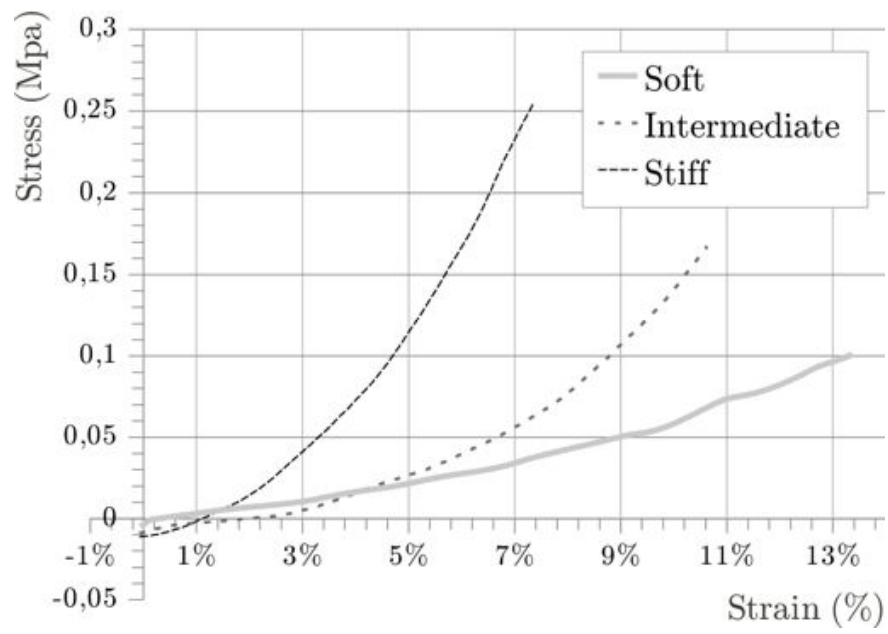370

371

372

373 <u>Fig. 5:</u> Plots of the strain/stress relationships measured for women. (R=ruptured,

374 U=unruptured, ACA = Anterior Cerebral Artery, ACM=Middle Cerebral Artery, ACI= Inter-

375 nal Carotid Artery, CPA= Cerebral Posterior Artery)

376

377

378

19

378

379

380

381   Fig.6: Mean strain/stress curves representing the biomechanical tissue classification.

382

383

383

Table 1: Summary of clinical, anatomical and biomechanical data of the sixteen cases studied. (U=Unruptured, R=Ruptured, U-PRS = Unruptured with pre-rupture symptoms, MCA =Middle Cerebral Artery, PComA = Posterior Communicating Artery, ICA = Internal Carotid Artery).The tissue classification (Soft/Rigid/Intermediate) is done according to the graphs shown in fig.4 et 5.

389

Female Subgroup	Location	Cumulative Documented Risk Factors	Aneurysm Status	Thickness (µm)	Biomechanical properties	C_{10} (MR3) MPa	C_{01} (MR3) MPa	C_{11} (MR3) MPa	Statistical Error
Aneurysm 3	MCA	0	**R**	420	Soft	0	0.0639	0.124	0.001
Aneurysm 4	ACA	2	**R**	300	Soft	0	0.0516	0.23	0.064
Aneurysm 16	ICA	1	**U-PRS**	380	Soft	0	0.04497	0.3077	0.00465
Aneurysm 6	PCA	5	**R**	450	Soft	0.02936	0	1.259	0.0355
Aneurysm 8	MCA	2	U	420	Intermediate	0.019057	0	2.196	0.0345
Aneurysm 11	MCA	5	U	390	Intermediate	0.0431	0	2.428	0.039
Aneurysm 10	ICA	5	U	310	Intermediate	0	0.0352	2.482	0.05
Aneurysm 15	PCA	1	U	680	Intermediate	0	0.06582	4.295	0.0433
Aneurysm 2	MCA	1	U	390	**Rigid**	0.376	0	**18.847**	0.033
Aneurysm 9	MCA	5	U	260	**Rigid**	0.2359	-0	**19.56**	0.049
Aneurysm 7	MCA	1	U	310	**Rigid**	0.7705	0	**32.149**	0.0067

390

391

392

393

Male Sub-group	Location	Cumulative Documented Risk Factors	Aneurysm Status	Thickness (µm)	Biomechanical properties	C_{10} (MR3) MPa	C_{01} (MR3) MPa	C_{11} (MR3) MPa	Stastistical Error
Aneurysm 5	ACA	1	**R**	330	Soft	0.1803	0	3.241	0.016
Aneurysm 13	ACA	1	**R**	290	Soft	0.9374	0	3.101	0.0267
Aneurysm 12	MCA	2	U	170	Intermediate	0.1951	0	14.987	0.0457
Aneurysm 14	MCA	1	U	200	Intermediate	0.1015	0	7.9232	0.04
Aneurysm 1	MCA	1	U	620	**Rigid**	0.2569	0	**12.265**	0.035

394

395

396
397

21

397

398

399

Table 2: Comparison of clinical and biomechanical parameters between the three identified tissue subgroups in the overall population.

n = 16	Aneurysmal wall biomechanical classification	n	Mean	p
Risk Factors	INTERMEDIATE	6	2.6	0.456
	SOFT	6	1.6	.
	RIGID	4	2	.
Wall Thickness	INTERMEDIATE	6	360	0.994
	SOFT	6	361	.
	RIGID	4	392	.
C10	INTERMEDIATE	6	0.0598	0.057
	SOFT	6	0.1911	.
	RIGID	4	0.3916	.
C01	INTERM	6	0.0168	0.792
	SOFT	6	0.0267	.
	RIGID	4	0.0322	.
C11	INTERM	6	5.71	<.001**
	SOFT	6	1.37	.
	RIGID	4	20.87	.

402

403

404

405

406

407

408

409

410

411

412

413

414

415

22

416

417

418

Table 3: Comparison of clinical data and biomechanical parameters between Ruptured and
Unruptured aneurysms in the overall population (male and female).

421

	Status	n	Mean	p
Risk factors	**Ruptured**	6	1.66	0.366
	Unruptured	10	2.4	.
Wall Thickness	**Ruptured**	6	0.36	0.918
	Unruptured	10	0,37	.
C10	**Ruptured**	6	0.19	0.404
	Unruptured	10	0.19	.
C01	**Ruptured**	6	0.026	0.757
	Unruptured	10	0.023	.
C11	**Ruptured**	6	1.377	0.004***
	Unruptured	10	11.78	

422

423

423

424

Table 4: Comparison of clinical data and biomechanical parameters between Ruptured and
Unruptured aneurysms in the female group.

	Status	n	Mean	p
Risk factors	**Ruptured**	4	2	0.516
	Unruptured	7	2.85	.
Wall Thickness	**Ruptured**	4	388	0.861
	Unruptured	7	392	.
C10	**Ruptured**	4	0.00734	0.200
	Unruptured	7	0.20637	.
C01	**Ruptured**	4	0.04012	0.279
	Unruptured	7	0.01443	.
C11	**Ruptured**	4	0.48	0.001**
	Unruptured	7	11.70	

427

428

428

429 <u>Table 5:</u> Comparison of clinical data and biomechanical parameters between Ruptured and

430 Unruptured aneurysms in the male group.

	Status	n	Mean	p
Risk factors	**Ruptured**	2	1	0.495
	Unruptured	3	1.3	.
Wall Thickness	**Ruptured**	2	309	0.638
	Unruptured	3	329	.
C10	**Ruptured**	2	0.558	0.638
	Unruptured	3	0.160	.
C01	**Ruptured**	2	-0.0001	0.638
	Unruptured	3	0.043	.
C11	**Ruptured**	2	3.17	0.058
	Unruptured	3	11.95	.

431

432

433

434

435

436

437

438

439

440

441

442

443

444

445

446

447

448

25

449

450

REFERENCES:

452

1. Wardlaw JM, White PM. The detection and management of unruptured intracranial aneurysms. *Brain*. 2000;123 (Pt 2):205-221

2. Sluzewski M, Bosch JA, van Rooij WJ, Nijssen PC, Wijnalda D. Rupture of intracranial aneurysms during treatment with guglielmi detachable coils: Incidence, outcome, and risk factors. *J Neurosurg*. 2001;94:238-240

3. Unruptured intracranial aneurysms--risk of rupture and risks of surgical intervention. International study of unruptured intracranial aneurysms investigators. *N Engl J Med*. 1998;339:1725-1733

4. Asari S, Ohmoto T. Natural history and risk factors of unruptured cerebral aneurysms. *Clin Neurol Neurosurg*. 1993;95:205-214

5. Wiebers DO, Whisnant JP, Sundt TM, Jr., O'Fallon WM. The significance of unruptured intracranial saccular aneurysms. *J Neurosurg*. 1987;66:23-29

6. Kyriacou SK, Humphrey JD. Influence of size, shape and properties on the mechanics of axisymmetric saccular aneurysms. *J Biomech*. 1996;29:1015-1022

7. Isaksen JG, Bazilevs Y, Kvamsdal T, Zhang Y, Kaspersen JH, Waterloo K, Romner B, Ingebrigtsen T. Determination of wall tension in cerebral artery aneurysms by numerical simulation. *Stroke*. 2008;39:3172-3178

8. Alnaes MS, Isaksen J, Mardal KA, Romner B, Morgan MK, Ingebrigtsen T. Computation of hemodynamics in the circle of willis. *Stroke*. 2007;38:2500-2505

9. Cebral JR, Castro MA, Appanaboyina S, Putman CM, Millan D, Frangi AF. Efficient pipeline for image-based patient-specific analysis of cerebral aneurysm hemodynamics: Technique and sensitivity. *IEEE Trans Med Imaging*. 2005;24:457-467

10. Radaelli AG, Augsburger L, Cebral JR, Ohta M, Rufenacht DA, Balossino R, Benndorf G, Hose DR, Marzo A, Metcalfe R, Mortier P, Mut F, Reymond P, Socci L, Verhegghe B, Frangi AF. Reproducibility of haemodynamical simulations in a subject-specific stented aneurysm model--a report on the virtual intracranial stenting challenge 2007. *J Biomech*. 2008;41:2069-2081

11. Hoi Y, Meng H, Woodward SH, Bendok BR, Hanel RA, Guterman LR, Hopkins LN. Effects of arterial geometry on aneurysm growth: Three-dimensional computational fluid dynamics study. *J Neurosurg*. 2004;101:676-681

12. Cebral JR, Mut F, Weir J, Putman C. Quantitative characterization of the hemodynamic environment in ruptured and unruptured brain aneurysms. *AJNR Am J Neuroradiol*. 2011;32:145-151

13. Cebral JR, Mut F, Weir J, Putman CM. Association of hemodynamic characteristics and cerebral aneurysm rupture. *AJNR Am J Neuroradiol*. 2011;32:264-270

14. Scott S, Ferguson GG, Roach MR. Comparison of the elastic properties of human intracranial arteries and aneurysms. *Can J Physiol Pharmacol*. 1972;50:328-332

15. Toth BK, Nasztanovics F, Bojtar I. Laboratory tests for strength paramaters of brain aneurysms. *Acta Bioeng Biomech*. 2007;9:3-7

16. Masson I, Fialaire-Legendre A, Godin C, Boutouyrie P, Bierling P, Zidi M. Mechanical properties of arteries cryopreserved at -80 degrees c and -150 degrees c. *Med Eng Phys*. 2009;31:825-832

17. Karmonik C, Diaz O, Grossman R, Klucznik R. In-vivo quantification of wall motion in cerebral aneurysms from 2d cine phase contrast magnetic resonance images. *Rofo*. 2010;182:140-150

18. Ogden GAHaRW. Biomechanical modelling at the molecular, cellular and tissue levels. *CISM Courses and Lectures, Springer: Wien, New York*. 2009;No. 508: 259-343

19. Marc André Meyers P-YC, Albert Yu-Min Lin, Yasuaki Seki. Biological materials: Structure and mechanical properties, review article. *Progress in Materials Science*. 2008;Volume 53:1-206

26

503 20. Oliver A. Shergold NAFaDR. The uniaxial stress versus strain response of pig skin and
504   silicone rubber at low and high strain rates. *International Journal of Impact Engineering*.
505   2006;Volume 32:1384-1402
506 21. Mooney M. A theory of large elastic deformation. *Journal of Applied Physics*.
507   1940;11:582-592.
508 22. Rivlin RS. Large elastic deformations of isotropic materials. *I. Fundamental concepts,*
509   *Philosophical Transactions of the Royal Society of London.Series A, Mathematical and*
510   *Physical Sciences*. 1948; 240:459-490.
511 23. Low SK, Zembutsu H, Takahashi A, Kamatani N, Cha PC, Hosono N, Kubo M, Matsuda
512   K, Nakamura Y. Impact of limk1, mmp2 and tnf-alpha variations for intracranial
513   aneurysm in japanese population. *J Hum Genet*. 2011
514 24. Crawford T. Some observations on the pathogenesis and natural history of intracranial
515   aneurysms. *J Neurol Neurosurg Psychiatry*. 1959;22:259-266
516 25. Frosen J, Piippo A, Paetau A, Kangasniemi M, Niemela M, Hernesniemi J, Jaaskelainen J.
517   Remodeling of saccular cerebral artery aneurysm wall is associated with rupture:
518   Histological analysis of 24 unruptured and 42 ruptured cases. *Stroke*. 2004;35:2287-2293
519 26. Watton PN, Ventikos Y, Holzapfel GA. Modelling the growth and stabilization of cerebral
520   aneurysms. *Math Med Biol*. 2009;26:133-164
521 27. Krings T, Willems P, Barfett J, Ellis M, Hinojosa N, Blobel J, Geibprasert S. Pulsatility of
522   an intracavernous aneurysm demonstrated by dynamic 320-detector row cta at high
523   temporal resolution. *Cen Eur Neurosurg*. 2009;70:214-218
524 28. Hayakawa M, Katada K, Anno H, Imizu S, Hayashi J, Irie K, Negoro M, Kato Y, Kanno
525   T, Sano H. Ct angiography with electrocardiographically gated reconstruction for
526   visualizing pulsation of intracranial aneurysms: Identification of aneurysmal protuberance
527   presumably associated with wall thinning. *AJNR Am J Neuroradiol*. 2005;26:1366-1369
528 29. Ishida F, Ogawa H, Simizu T, Kojima T, Taki W. Visualizing the dynamics of cerebral
529   aneurysms with four-dimensional computed tomographic angiography. *Neurosurgery*.
530   2005;57:460-471; discussion 460-471
531 30. MacDonald DJ, Finlay HM, Canham PB. Directional wall strength in saccular brain
532   aneurysms from polarized light microscopy. *Ann Biomed Eng*. 2000;28:533-542
533 31. Zhang C, Villa-Uriol MC, De Craene M, Pozo JM, Frangi AF. Morphodynamic analysis of
534   cerebral aneurysm pulsation from time-resolved rotational angiography. *IEEE Trans Med*
535   *Imaging*. 2009;28:1105-1116
536 32. Balocco S, Camara O, Vivas E, Sola T, Guimaraens L, Gratama van Andel HA, Majoie CB,
537   Pozo JM, Bijnens BH, Frangi AF. Feasibility of estimating regional mechanical properties
538   of cerebral aneurysms in vivo. *Med Phys*. 2010;37:1689-1706
539 33. Zhao X, Raghavan ML, Lu J. Identifying heterogeneous anisotropic properties in cerebral
540   aneurysms: A pointwise approach. *Biomech Model Mechanobiol*. 2011;10:177-189

541

542

543

27

543

544

Conflict of interest statement

All authors do not have any financial and personal relationships with other people or organi-

sations that could inappropriately influence this work.

548

549

549

555